Author(s): Vehviläinen, T. T. & Ganchenkova, M. G. & Oikkonen, L. E. & Nieminen, Risto M.

Title: Hydrogen interaction with fullerenes: From C[sub 20] to graphene

Year: 2011

Version: Final published version

Please cite the original version:

Vehviläinen, T. T. & Ganchenkova, M. G. & Oikkonen, L. E. & Nieminen, Risto M. 2011. Hydrogen interaction with fullerenes: From C[sub 20] to graphene. Physical Review B. Volume 84, Issue 8. 085447/1-7. ISSN 1550-235X (electronic). DOI: 10.1103/physrevb.84.085447.

Hydrogen interaction with fullerenes: From C_{20} to graphene

T. T. Vehviläinen,* M. G. Ganchenkova, L. E. Oikkonen, and R. M. Nieminen
COMP/Department of Applied Physics, School of Science, Aalto University, P.O. Box 11100, FI-00076 Aalto, Espoo, Finland
(Received 7 February 2011; published 30 August 2011)

The paper presents a systematic study of the trends in the interaction of hydrogen with carbon fullerenes versus their curvature, where graphene is taken as the limit of zero curvature. The efficiency of hydrogen incapsulation in fullerenes, penetration into them, and adsorption on their surface are analyzed and discussed. The effects on magnetism are also considered; in particular, it is shown that hydrogen adsorption to some fullerenes induces magnetism to initially nonmagnetic systems. In addition, highly hydrogen-saturated fullerenes are examined and the suitability of fullerenes for hydrogen storage is discussed.

DOI: 10.1103/PhysRevB.84.085447 PACS number(s): 68.35.bp, 68.43.Bc, 33.15.Fm, 88.30.R−

I. INTRODUCTION

The discovery of fullerenes in 1985[1] led to a rapid rise in carbon research and prepared the way for finding other carbon nanomaterials, including nanotubes, graphene, and other exotic structures. Fullerenes, which are zero-dimensional nano-objects, are not merely theoretically interesting but offer many potential applications. Among the fields of application of fullerenes have been drug delivery[2] and hydrogen storage, which require detailed information about the hydrogenation of fullerene molecules.

In the search for substitutes for the rapidly diminishing supply of fossil fuels, hydrogen is considered as a particularly suitable energy carrier due to its cleanliness and abundance in nature. However, the implementation of hydrogen technology is hindered by the lack of convenient, cost-effective storage systems.[3] Among the various possibilities considered, materials-based storage of hydrogen stands out as a particularly promising solution. Materials ranging from metal hydrides to carbon nanostructures have been studied, and while metal hydrides have reached the highest volumetric densities of hydrogen, carbon-based materials offer potential for more lightweight storage.[4,5]

Of the various carbon nanostructures that exist in nature,[6] carbon nanotubes have been investigated for hydrogen storage the most.[7–10] Along with nanotubes, carbon fullerenes have been considered as well. Fullerenes offer versatile possibilities for hydrogen storage: in addition to being adsorbed on the outer surface of fullerenes, hydrogen can also be accumulated inside them.[11] However, it should be kept in mind that in order to be useful in hydrogen storage applications the material should demonstrate a reversible storage capacity at the ambient pressure and temperature. Hydrogen chemisorption on carbon structures may partially fulfill this requirement; since the C-H bond is weaker than the C-C bond, an increase in temperature will break the C-H bond and dehydrogenate the structure without destroying it.

Experimentally, there have been several attempts to saturate fullerenes with hydrogen. In fact, some fullerenes can even be produced directly with hydrogen coverage; for instance, C_{20} was first observed experimentally when hydrogen atoms in $C_{20}H_{20}$ were replaced by weakly bound Br atoms followed by debromination.[12] Unfortunately, in most cases, hydrogenation of the carbon nanostructure is more cumbersome. In particular, producing endohedrally doped fullerenes, often requires extreme reaction conditions and the use of such methods as ion bombardment, high-pressure, or high-temperature techniques.[13] A less brutal and more efficient alternative has been the *molecular surgery* method, where the fullerene cage has been opened by chemical treatment, and hydrogen has been inserted inside.[14,15]

In previous studies investigating the suitability of fullerenes for hydrogen storage, the C_{60} molecule has been most often considered. In contrast, there exist only fragmented studies of other fullerenes. In this paper, we carry out a systematic study of the interaction of hydrogen with different-sized fullerenes using thorough *ab initio* simulations. We will establish trends between parameters characterizing the interaction and the fullerene size.

The paper is organized as follows. Section II contains the methodology part, which describes the settings used for the calculations. Then the results obtained from the *ab initio* simulations are presented and discussed. Section III A describes in detail how hydrogen can be accumulated in fullerenes, and Sec. III B describes the adsorption of hydrogen on the surface of the fullerene. Section III C discusses hydrogen molecule dissociation over fullerenes, and Sec. III D briefly discusses the properties of highly saturated fullerene surfaces. Finally, in Sec. IV, conclusions are drawn on the interaction of hydrogen with the fullerenes.

II. METHODS

The calculations have been performed using the plane-wave-based code VASP,[16,17] implementing the spin-polarized density-functional theory (DFT). The calculations were carried out in the generalized-gradient approximation (GGA) of Perdew, Burke, and Ernzerhof (PBE).[18] The core ($1s^2$) electrons were described by the projector-augmented-wave (PAW) method.[19] The cutoff energy of 400 eV for the plane-wave basis set was found to give energy convergence within a few meV. For the irreducible Brillouin-zone integration, the Monkhorst-Pack[20] $4 \times 4 \times 4$ **k**-point sampling for C_{20} molecule systems and $2 \times 2 \times 2$ mesh for C_{60} molecule systems was used together with appropriate Fermi smearing. Supercells were constructed with adequate vacuum space of at least 8 Å in each cartesian direction in order to minimize the spurious interaction of the fullerene with its images in neighboring supercells.

III. RESULTS AND DISCUSSION

In principle, hydrogen can be accumulated in a fullerene either by forming a bond with a carbon atom outside or inside the cage, or by simply getting trapped inside the hollow fullerene. These three possible configurations with the corresponding schematic energy diagram are illustrated in Figs. 1(a)–1(d). In this study, we consider how the size of the fullerene affects hydrogen adsorption. A number of fullerenes C_m, where $m = 20$–60, have been considered. The case of graphene is considered as the limit of zero curvature.

A. Hydrogen accumulation inside fullerenes

Let us first consider the case of hydrogen accumulation inside fullerenes. There exist two possible configurations: the hydrogen atom can either be confined to the center of the fullerene or chemisorbed to the inner surface of the cage as shown in Figs. 1(b) and 1(c). Total-energy calculations will ultimately show whether these configurations are truly energetically favorable. The interaction energy between the fullerene and hydrogen atom was calculated as follows:

$$E_{\text{int}} = E_{\text{C}_m\text{H}} - \left(E_{\text{C}_m} + E_{\text{H}}\right), \tag{1}$$

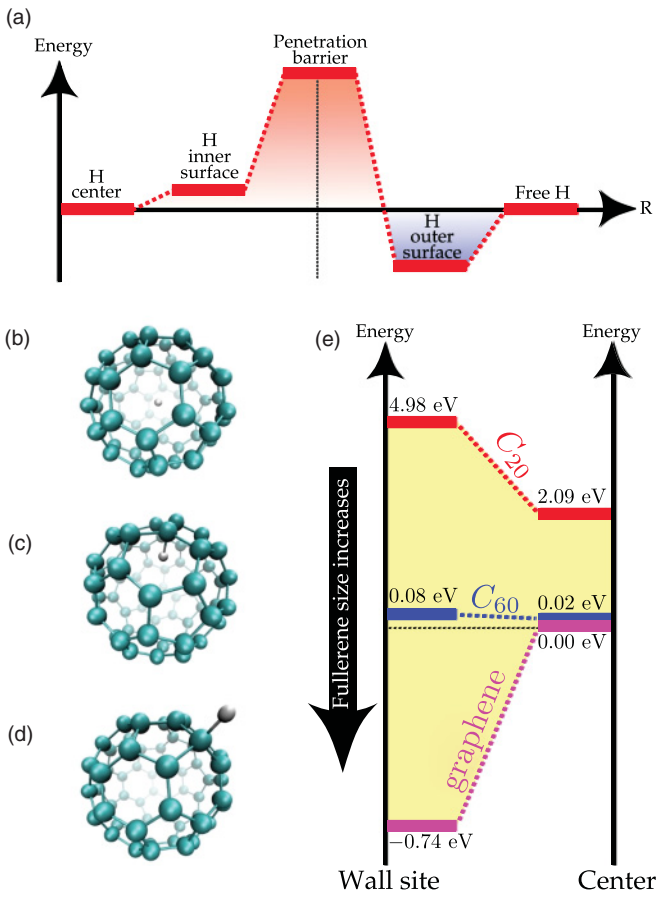

FIG. 1. (Color online) (a) Schematic energy diagram of the interaction energy between hydrogen atom and fullerene cage. (b) Hydrogen atom at the center of the fullerene and (c) chemisorbed from the inside. (d) Hydrogen atom chemisorbed outside the fullerene. (e) Schematic energy diagram for H atom adsorbed to the inner wall and H located at the center of the fullerene.

where $E_{\text{C}_m\text{H}}$ denotes the total energy for the system consisting of a C_m fullerene (m being the number of carbon atoms constituting the fullerene) with a H atom, E_{C_m} is the energy of the isolated fullerene C_m, and E_{H} is the energy of an isolated hydrogen atom.

For hydrogen confined inside the fullerene molecule, the total energies of the C_mH^{center} system were computed such that the hydrogen atom was positioned at the center of the fullerene, see Fig. 1(b). The interaction energy between the hydrogen and fullerene is shown in Fig. 2(a). It was found that when $m \geqslant 60$, the whole system C_mH^{center} has essentially the same energy as when C_m and H are far from each other. In other words, the hydrogen atom behaves like a free atom at the center of the fullerene ($m \geqslant 60$), confirming results from previous studies for the case of C_{60}.[21] For smaller fullerenes ($m \leqslant 60$), adsorption to the center is more favorable than adsorption to the inner wall, see energy diagram in Fig. 1(e). The curvature of the inner surface creates a repulsive interaction between the surface of the fullerene and hydrogen atom, and, therefore, there always exists an energy minimum at the center of the fullerene molecule where hydrogen can be confined. When the fullerene size decreases, the repulsive interaction between hydrogen confined to the center and the fullerene increases rapidly, reaching 2.09 eV for C_{20}, see Fig. 2(a). This indicates that these states are not likely to form.

The H atom encapsulation at the center of the fullerene can affect the total magnetic moment of the fullerene, see Fig. 2(b). In most of the cases, it changes the magnetic moment by $1\mu_B$ for the initially nonmagnetic molecules. However, some exceptions exist like C_{30}, for which H increases the magnetic moment up to $1.7\mu_B$. Some of the fullerene molecules are intrinsically magnetic; C_{20} and C_{28} have magnetic moments of $1.7\mu_B$ and $3.9\mu_B$, respectively. For these magnetic fullerenes, H encapsulation changes the magnetic moment differently; for C_{20}, it increases by $1\mu_B$, whereas for C_{28}, it decreases by the same amount. The magnetic properties of fullerene

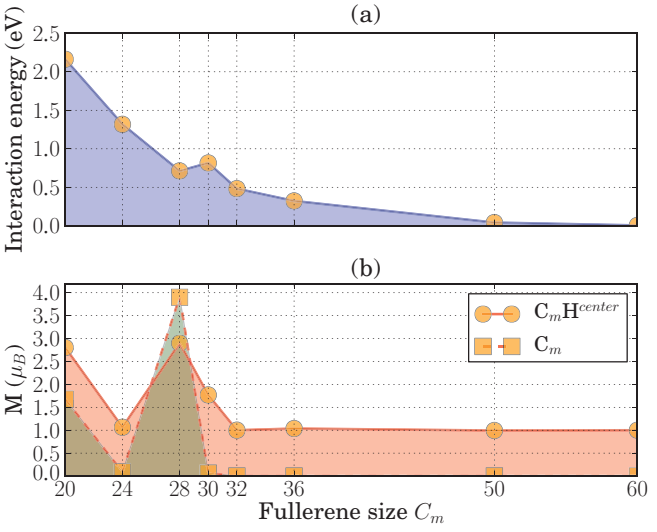

FIG. 2. (Color online) (a) Interaction energy of the H atom confined at the center of a fullerene C_m and (b) magnetic moment of the fullerene C_m and C_mH system, where m is the number of carbon atoms.

TABLE I. Values for adsorption energy (Eq. 1) for the chemisorbed state of the hydrogen atom inside C_{20} and C_{60} fullerenes and graphene as a reference.

System	E_{ads} (eV)	Ref.
C_{20}	4.98	this work
C_{60}	0.08	this work
	0.5	DFTB[a] [21]
	0.3	Brenner[b] [22]
Graphene	−0.74	this work
	−0.83	DFT [23]
	−0.75–0.84	DFT[c] [24]

[a]Density-functional-based tight-binding method.
[b]Semiempirical many-body potential.
[c]Value depends on the supercell used in calculations.

molecules have been previously studied using quantum Monte Carlo methods for C_{20} [25] and C_{60} [26] molecules. Based on the Hubbard model used in Refs. 25–27, strong correlation effects have been suggested to be important as a possible source of magnetism for fullerene molecules.

In addition to the confined state at the center of the fullerene, the hydrogen atom can also be chemisorbed to the inner surface of the fullerene cage, see Fig. 1(c). Nevertheless, this state is found to be energetically less favorable than confinement at the center of the fullerene ($m \leqslant 60$). For instance, the adsorption energy in the case of C_{60} is 0.08 eV. As can be seen in Table I, the GGA PAW approximation gives smaller values for the chemisorbed state of the hydrogen inside C_{60} fullerene compared to density-functional tight-binding (DFTB) and Brenner potential based calculations.[21,22] For example, DFTB gives a value of 0.5 eV, which is significantly larger than the value of 0.08 eV calculated in this study. Similar to the case of confinement at the center, the adsorption energy is found to increase to 4.98 eV when the fullerene size decreases to C_{20}.

These results show that, generally speaking, hydrogen can be accumulated inside fullerenes whose size is equal to or larger than C_{60}. Smaller fullerenes are too confined to be able to hold a hydrogen atom inside; the interaction between fullerene walls and the hydrogen atom becomes too disruptive.

Hydrogen accumulation inside fullerenes does not, however, depend only on the favorable energetics of the final configuration. In order for the hydrogen atom to enter the fullerene cage, it has to overcome a potential barrier, the height of which is unknown *a priori*. This energy barrier can hinder the passage of the hydrogen into the fullerene. We examined this barrier for the smallest feasible H carrier fullerene, namely, C_{60}.

Calculations were performed by varying the distance of the hydrogen atom from the center of the fullerene, where the movement of the H atom is restricted, to the line passing strictly through the center of one facet. The hydrogen atom was let to move freely in the plane parallel to the fullerene facet. The hydrogen penetrations through the hexagonal and pentagonal rings were considered separately.

The calculated energy barriers are presented in Fig. 3 and Table II. When the hydrogen atom is moved toward the center of the fullerene through the hexagonal ring, it faces an energy barrier of 2.57 eV. The value for the energy barrier is smaller than the previously published values, which have been mostly calculated by semiempirical methods, as listed in Table II. When the hydrogen atom enters the fullerene through the pentagonal ring, the barrier is even higher, 3.24 eV. From Fig. 3, we can see that the saddle points are located 0.2 and 0.4 Å away from the fullerene pentagonal and hexagonal facets, respectively, and that there also exists a small mimimum ≈0.8 Å away from a facet inside the fullerene. For comparison, Seifert *et al.*[21] using the DFTB method have obtained a larger value for the barrier, 3.7 eV (see Table II).

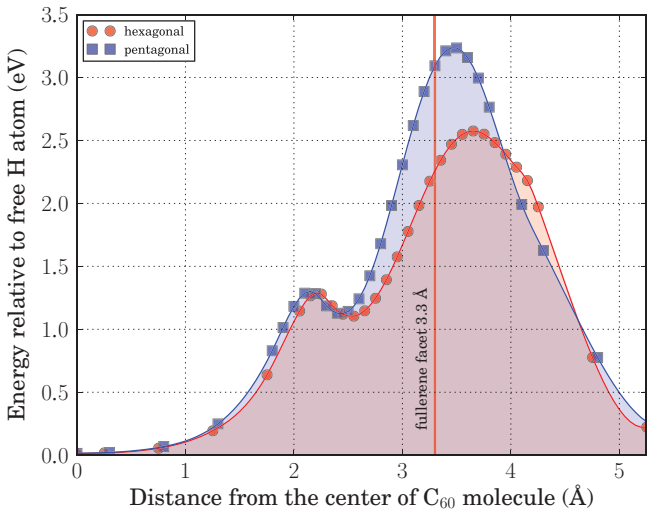

FIG. 3. (Color online) Penetration barrier for the hydrogen atom entering the C_{60} fullerene. Both facets are situated ≈3.3 Å from the center of the fullerene.

Based on these considerations, hydrogen accumulation inside fullerenes by penetrating through the cage wall does not seem likely in practice due to the high penetration barrier, which is at least 2.57 eV for C_{60} and increases to 3.4 eV for a graphene sheet.

Nevertheless, we cannot completely dismiss the idea of H accumulation inside fullerenes because endohedral hydrogen fullerenes can still be produced using the molecular surgery method.[14,15] Using DFT-based molecular dynamics (MD) simulations, Pupysheva *et al.*[14] have shown that a maximum number of $n = 58$ hydrogen atoms inside C_{60} fullerene can form a metastable structure. If $n \geqslant 30$, some hydrogen atoms

TABLE II. Values for the energy barriers for the hydrogen atom moving through a hexagonal/pentagonal ring of C_{60}.

Method	Hex. (eV)	Pen. (eV)	Ref.
GGA, PAW	2.57	3.24	this work
DFTB	3.0	3.7	Ref. 21
PM3[a]	3.01	···	Ref. 28
B3LYP, 6-31G[b]	3.27	···	Ref. 28
Brenner	3.9	···	Ref. 22

[a]Parametric model number 3, a semiempirical method that neglects differential diatomic overlap integrals.
[b]Becke's three-parameter hybrid functional using the Lee, Yang, and Parr correlation functional[29] with the 6-31G basis set.

TABLE III. Adsorption energy for hydrogen atom on different fullerenes. NP and NH denote pentagonal and hexagonal facets next to adsorption site, h is elevation for carbon atom below hydrogen, measured from the plane where three carbon atoms next to adsorption site define before hydrogen adsorption (see inset in Fig. 3) and s1, . . . ,s6 are adsorption sites on the fullerene surface, d(C-H) is the carbon-hydrogen bond length, and W is the number of adsorption sites on the surface.

Structure	h (Å)	NH	NP	d(C-H)	E_{ads} (eV)	M (μ_B)	W
$C_{20}H$	0.519	0	3	1.096	−4.10	0.49	20
$C_{24}H^{s1}$	0.525	1	2	1.099	−3.88	0	12
$C_{24}H^{s2}$	0.420	0	3	1.100	−3.58	0	12
C_{24}^{ave}	0.472				−3.73		
$C_{28}H^{s1}$	0.433	0	3	1.103	−4.37	2.84	4
$C_{28}H^{s2}$	0.441	1	2	1.104	−3.43	2.94	12
$C_{28}H^{s3}$	0.422	1	2	1.102	−4.04	2.86	12
C_{28}^{ave}	0.431				−3.82		
$C_{30}H^{s1}$	0.326	2	1	1.103	−3.06	0	10
$C_{30}H^{s2}$	0.444	1	2	1.100	−3.82	0	10
$C_{30}H^{s3}$	0.513	0	3	1.099	−3.82	0	10
C_{30}^{ave}	0.427				−3.57		
$C_{32}H^{s1}$	0.458	0	3	1.101	−2.90	0.68	2
$C_{32}H^{s2}$	0.431	1	2	1.104	−2.31	0	6
$C_{32}H^{s3}$	0.422	1	2	1.104	−2.55	0.85	6
$C_{32}H^{s4}$	0.391	1	2	1.105	−2.61	0.46	6
$C_{32}H^{s5}$	0.358	2	1	1.106	−2.25	0.28	6
$C_{32}H^{s6}$	0.396	1	2	1.104	−2.65	0	6
C_{32}^{ave}	0.403				−2.50		
$C_{36}H^{s1}$	0.318	2	1	1.107	−2.22	0.65	12
$C_{36}H^{s2}$	0.400	1	2	1.103	−3.44	0.89	12
$C_{36}H^{s3}$	0.422	1	2	1.105	−2.89	0.60	12
C_{36}^{ave}	0.380				−2.85		
$C_{50}H^{s1}$	0.283	2	1	1.112	−2.21	0	10
$C_{50}H^{s2}$	0.313	2	1	1.110	−2.55	0	10
$C_{50}H^{s3}$	0.309	2	1	1.110	−2.41	0	20
$C_{50}H^{s4}$	0.385	1	2	1.105	−3.21	0	10
C_{50}^{ave}	0.320				−2.56		
$C_{60}H$	0.283	2	1	1.111	−2.01	0	60
Graphene	0.000	3	0	1.127	−0.74	0	–

form covalent bonds with carbons of the fullerene cage, which weakens the fullerene C-C bonds.

B. Hydrogen atom chemisorption outside the fullerene

The penetration barriers discussed in the previous section were obtained by moving the hydrogen atom strictly along the perpendicular axis passing through a facet center. However, a penetration will not occur if the hydrogen atom is not placed exactly on this axis or if it does not have high enough initial energy. Instead, the hydrogen will shift toward one of the closest carbon atoms constituting the facet ring and form a bond with it, see Fig. 1(d). The bond formation will slightly distort the fullerene cage outward, but the energy gain due to the favorable hybridization will still dominate over the strain energy.

The calculated adsorption energy (1) for H chemisorbed on the outer fullerene surface on the top site over the

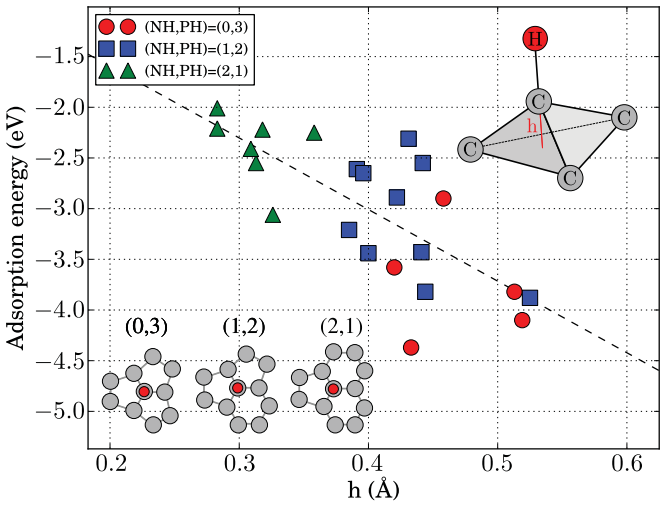

FIG. 4. (Color online) Adsorption energy for hydrogen atom chemisorbed to the surface of different fullerene molecules. Adsorption data for each fullerene is listed in Table III.

C atom is presented in Table III and Fig. 4 for different fullerenes. H adsorption is always favorable regardless of fullerene size. Nevertheless, the adsorption energy increases nonmonotonically with the increase of the fullerene size: from −4.10 eV for a C_{20} molecule to −2.01 eV for C_{60} (in agreement with −2.13 eV calculated by Okamoto[11]) and then −0.74 eV for a graphene plane (in agreement with −0.83 eV calculated by Ferro *et al.*[23]). It should be noted that, for nonspherical fullerenes such as C_{32} or C_{36}, several nonequivalent sites exist for H adsorption and therefore the adsorption energy is site dependent, see Table III. Adsorption sites on fullerenes, which are smaller than C_{60}, can be assigned to three categories based on the number of hexagonal (NH) and pentagonal (NP) facets next to the adsorption site. There always exists at least one pentagonal facet neighboring the adsorption site and therefore (NH,NP) can have values (0,3), (1,2), and (2,1) as shown in the insert of Fig. 4. If all rings are pentagonal (0,3), the local geometry of the adsorption site is sharply peaked and adsorption is energetically highly favorable. Hexagonal facets will tend to keep the surface flat and therefore binding to the (2,1) sites is the weakest. In general, fullerene sizes have a large effect on how strongly H atoms are adsorbed on the surface; the smaller the fullerene, the more strongly the hydrogen atoms are attached to the surface. However, there exist large deviations in adsorption energies between different adsorption sites on the same fullerene molecule, see Table III. For example in the C_{36} fullerene, the adsorption energy difference between sites s1 and s2 is 1.22 eV.

As we have shown in Sec. III A, fullerene molecules $\geqslant C_{30}$ without defects or adsorbates are not magnetic [see Fig. 2(b)]. Usually, the magnetization of carbon nanostructures is associated with defects such as vacancies,[30] adatoms,[31] transition metal atoms,[32] or negative Gaussian curvature.[33] Hydrogen has been demonstrated to induce magnetism also in nanostructures with defective surfaces[34] or high hydrogen coverages.[35]

We have observed that already a single H atom adsorption to fullerenes C_{32} and C_{36} induces a magnetic moment. As we see from Table III, hydrogen adsorption to some sites

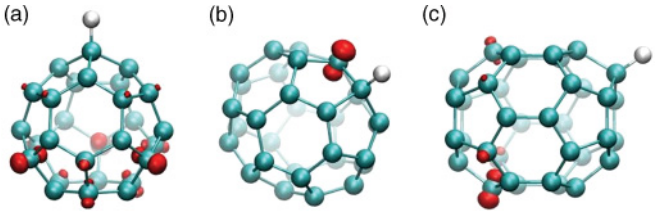

FIG. 5. (Color online) Spin-density isosurface for (a) C_{28} at 0.20 $e/Å^3$, (b) C_{32} at 0.16 $e/Å^3$, and (c) C_{36} at 0.10 $e/Å^3$.

induces a magnetic moment varying from 0.28 to 0.89 μ_B for a $C_{32}H^{s5}$ and $C_{36}H^{s2}$, respectively, while fullerenes C_{24}, C_{30}, C_{50}, and C_{60} remain nonmagnetic after hydrogen adsorption. Spin-density plots show that the highest spin-density location depends on the fullerene, see Fig. 5. In some cases, it is located on the opposite side of the hydrogen adsorption site, but can also be located on the carbon atom next to the adsorption site.

H adsorption to initially magnetic fullerenes, such as C_{20} and C_{28}, reduces the value of the magnetic moment by $1\mu_B$. Among fullerenes considered in this study, the largest magnetic moment is obtained for H on the C_{28} fullerene having a magnetic moment of $2.9\mu_B$, while the pure C_{28} fullerene has a magnetic moment of $3.9\mu_B$.

Magnetization also exists in some fullerenes with multiple hydrogen atoms adsorbed to the surface. For example, two hydrogen atoms adsorbed to the site s1 on C_{28} will reduce the magnetic moment to $1.8\mu_B$ and three atoms to $0.8\mu_B$, while the magnetic moment for one hydrogen on site s1 is $2.84\mu_B$. The largest spin density is located on the opposite site of hydrogen adsorption, see Fig. 6.

C. Hydrogen-molecule adsorption to fullerene surface

In the previous section, the interaction of atomic hydrogen with a fullerene was considered. However, experiments most commonly deal with molecular hydrogen. The H_2 molecule must dissociate before adsorption to the fullerene surface can occur, which creates a barrier for the adsorption process.

On the fullerene surfaces, there are various different positions over which the H_2 molecule can dissociate. The values for the dissociation barriers depend both on the size of the fullerene and the local geometry near the dissociation site, i.e., whether the H-H bond is parallel to the C-C bond ($^{\text{bond}}$), parallel to opposite C atoms on the hexagonal facet ($^{\text{hex}}$), or parallel to some other C-C pair. As in the case of H atom adsorption, the larger the curvature of the fullerene, the more reactive the surface is and the more easily the H_2 molecule dissociates and H atoms adsorb to the surface, see Fig. 7. Indeed, while above the C_{20} fullerene, the barrier for hydrogen molecule dissociation is 0.9 eV, it increases to 3.7 eV for C_{60}^{hex} and 4.2 eV for graphene$^{\text{bond}}$. Comparing to carbon nanotubes (CNT), for example CNT(10,10) and CNT(8,8) as considered in Ref. 36, the dissociation of H_2 molecule over the surface requires more energy than that for the case of C_{20} and goes easier over the C atom having a dangling bond. This is also confirmed by our calculations done earlier for CNT(10,0). In this case, the dissociation energies for H_2 are 2.0 and 4.0 eV over hexagon and above C-C bond configuration, respectively. Highly curved surfaces bind hydrogen atoms very strongly, which can be seen from the calculated adsorption-energy values for H_2 molecule; they are −3.8, −0.6 , 1.7, and 1.8 eV for C_{20}^{bond}, C_{60}^{hex}, graphene$^{\text{bond}}$, and graphene$^{\text{hex}}$, respectively. The reaction paths for the dissociation of the H_2 molecule

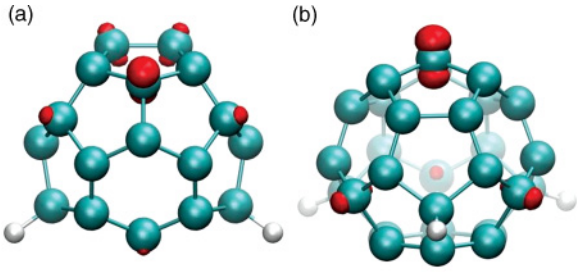

FIG. 6. (Color online) Spin-density isosurface for (a) C_{28} with two hydrogen atoms on surface (2 × site s1) at 0.15 $e/Å^3$ and (b) C_{28} with three hydrogen atoms on surface (3 × site s1) at 0.10 $e/Å^3$.

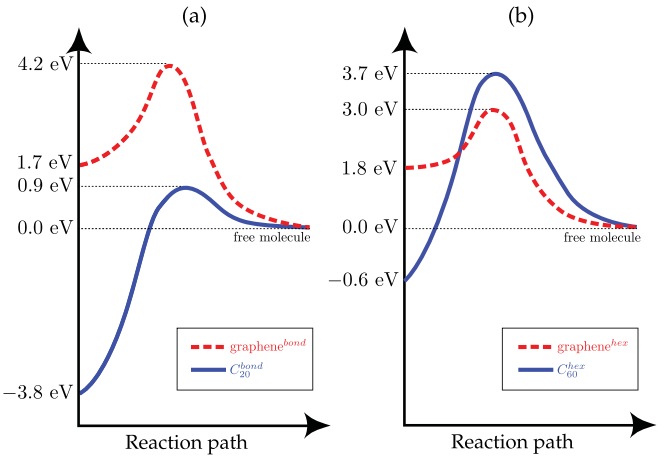

FIG. 7. (Color online) Hydrogen molecule dissociation and adsorption above C-C bond (a) and above hexagonal facet (b) on the fullerene and graphene outer surfaces.

TABLE IV. Adsorption energy for a hydrogen atom on C_mH. The second hydrogen atom is adsorbed next to the hydrogen atom. Sites (i,j) are adsorption sites as denoted in Table III, M is the total magnetic moment of the system and E_i and E_j denote adsorption energies for second hydrogen adsorption to sites i and j, respectively. ΔE^{ads} ($\Delta E_i^{\text{ads}} = \Delta E_j^{\text{ads}}$) is the adsorption-energy difference between E_i and adsorption energy for one hydrogen on site i, $\Delta E^{\text{ads}} = E(C_mH^{Si}) - E_i$.

Structure	M (μ_B)	site (i,j)	E_j	E_i	ΔE^{ads}
$C_{20}H_2$	0.0	1,1	−4.20		−0.08
$C_{36}H_2$	0.0	1,2	−3.76	−2.54	−0.31
$C_{36}H_2$	0.0	0,1	−2.29		−0.06
$C_{36}H_2$	0.55	2,3	−2.87	−3.43	0.01
$C_{36}H_2$	0.0	3,3	−3.42		0.02
$C_{60}H_2$	0.0	1,1	−3.38		−1.37
$C_{60}H_2$	0.0	1,1	−2.59		−0.58

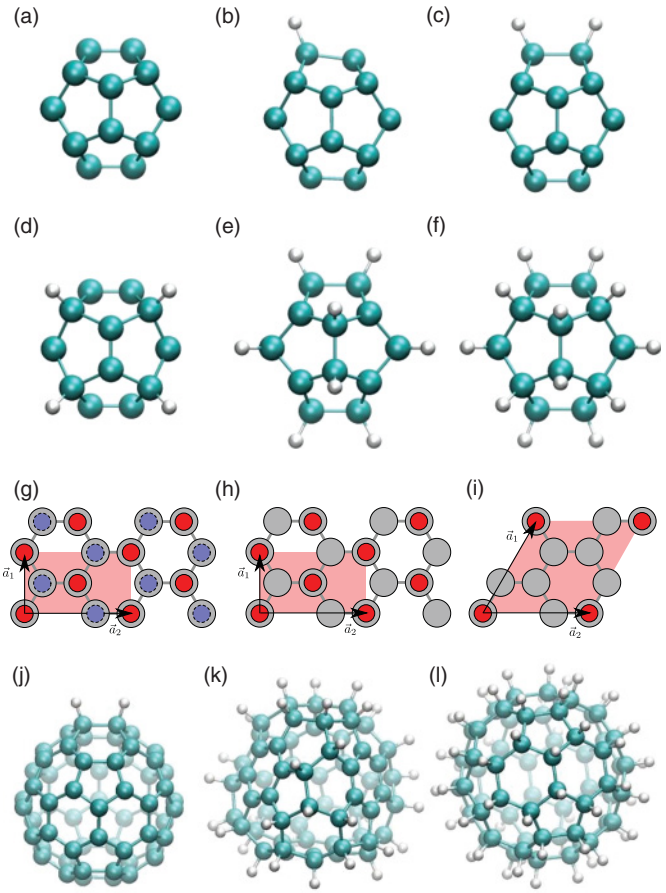

FIG. 8. (Color online) Configurations of H saturated fullerene and graphene surfaces: (a) C_{20}, (b) $C_{20}H$, (c) $C_{20}H_2$, (d) $C_{20}H_8$, (e) $C_{20}H_{12}$, (f) $C_{20}H_{20}$, (g) Graphene 1 ML, (h) Graphene 1/2 ML, (i) Graphene 1/6 ML, (j) $C_{60}H_2$, (k) $C_{60}H_{36}$, and (l) $C_{60}H_{60}$. In graphene pictures, dashed circles represents hydrogen atoms on the other side of graphene sheet and polygon represents supercell used in calculations.

were calculated using the climbing-image nudged-elastic-band method.[37,38]

When two hydrogen atoms are adsorbed on the surface, it is possible for the hydrogens to recombine and form H_2 molecule, which desorbs from the fullerene. The energy required for H_2 molecule to desorb is 4.7, 4.3, 2.5, and 1.2 eV for C_{20}^{bond}, C_{60}^{hex}, graphene^{bond}, and graphene^{hex} surfaces, respectively. Thus, the adsorption is more effective the smaller fullerene is, whereas the H_2 molecule recombination and desorption goes easier the flatter surface is.

D. Formation of a highly H-saturated fullerene: C_{20} and C_{60} versus graphene

Hydrogen adsorbed on C_mH has an effect on the adsorption energy of a second H atom of the same fullerene if they form a nearest-neighbour configuration. At the same time, this energy is dependent on the nearest-neighbour configuration type as specified in Table IV. The adsorption-energy change due to the hydrogen atom adsorbed to the surface for all fullerenes is given in Table IV. The adsorption-energy change is largest for the C_{60} fullerene, where ΔE^{ads} is -1.37 or -0.58 eV depending on the surface configuration of the two hydrogen atoms. This indicates the binding between hydrogen atoms and formation of hydrogen nearest-neighbour pairs on the surfaces.

Due to the high reactivity of the fullerene molecules, smaller than C_{60}, with respect to hydrogen atoms, one can expect the formation of a C_mH_n molecule, where $n = 1, \ldots, m$. To examine the formation of a highly H-saturated fullerene molecule, we have calculated the dependence of the adsorption energy of the H atom on the number of H atoms adsorbed on the C_{20} and C_{60} fullerenes, which are taken as example cases for highly saturated fullerenes. For comparison, one monolayer (ML) hydrogen coverage, also known as graphane[39,40] (1/2 ML on both sides of graphene), 1/2 ML, and 1/6 ML hydrogen coverages are calculated for the graphene surface, see Fig. 8. As we can see from Table V, hydrogen has a smaller adsorption energy on the C_{20} surface compared to C_{60} surface or graphene. We expect that similar to the case of single hydrogen atom adsorption, the curvature of the fullerene has a strong effect on the adsorption of multiple hydrogens and smaller fullerenes bind hydrogens more efficiently. It should be noted that the adsorption energy decreases nonmonotonically when the number of H atoms increases. For C_{20}, in particular, it decreases, first, from -4.11 to -3.11 eV when the total number of H atoms adsorbed at the surface, n, increases from 1 to 12 and then increases when $n > 12$. This can be explained as the strain effect, which is introduced by the H atoms adsorbed on the surface, and is more pronounced with the larger curvature of the cage. A similar phenomenon is observed also for the C_{60} fullerene. For graphene, single H adsorption, 1/2 ML, and 1/6 ML coverages are energetically almost equal. Furthermore, both coverages exhibit magnetic moments, which are 1.0 and $2.0\mu_B$ for 1/6 ML and 1/2 ML of H on graphene, respectively. For 1/2 ML hydrogen coverage, the spins are found to be located at two carbon atoms, which are not hydrogenated, in agreement with earlier calculations.[35] However, fully saturated graphane is energetically very favourable compared to other coverages. This is mainly due to the hydrogen-induced change

TABLE V. Adsorption energy per atom for multiple hydrogen atoms on C_{20} and C_{60} molecule and graphene. Configurations can be seen in Fig. 8.

Structure	E_{ads} (eV)	M (μ_B)	Structure	E_{ads} (eV)	M (μ_B)	Structure	E_{ads}(eV)	M (μ_B)
$C_{20}H$	-4.11	0.49	$C_{60}H$	-2.01	0.0	Graphene 1 ML	-2.47	0.0
$C_{20}H_2$	-4.15	0.0	$C_{60}H_2$	-2.70	0.0	Graphene 1/2 ML	-0.62	1.98
$C_{20}H_8$	-3.72	0.0	$C_{60}H_{36}$	-2.75	0.0	Graphene 1/6 ML	-0.69	0.99
$C_{20}H_{12}$	-3.11	0.0	$C_{60}H_{60}$	-2.44	0.0	Graphene H	-0.74	0.0
$C_{20}H_{20}$	-3.55	0.0						

of hybridization for all C atoms in the sheet to sp^3 bonding, which keeps the surface flat while allowing each C atom to relax locally to a typical diamond-like configuration.

IV. SUMMARY AND DISCUSSION

Based on our calculations, we conclude that hydrogen accumulation inside fullerenes is not likely due to the high penetration barrier. However, H adsorption on the fullerene outer surface is possible; the adsorption of atomic H occurs without a barrier, and even molecular H_2 can be adsorbed provided that the activation energy for the dissociation is supplied. The adsorption energy for hydrogen varies nonmonotonically with fullerene size. The smaller the fullerene the smaller is the adsorption energy as well as the dissociation energy of H_2 molecule over the surface. Some hydrogen-decorated fullerenes have magnetic ground states. While in previous studies magnetism of carbon nanostructure has been shown to arise from defects,[30,31] transition-metal-atom doping,[32] negative Gaussian curvature,[33] or high hydrogen coverages,[35] we have shown that a single hydrogen atom can make a fullerene molecule magnetic and induce magnetic moments such as $0.85\mu_B$ in $C_{32}H$ molecule. We have also observed that magnetization does not necessarily vanish with increasing number of hydrogen atoms adsorbed to the surface of the fullerene.

ACKNOWLEDGMENTS

This work was supported by the Academy of Finland through its Center of Excellence Program (2006–2011) and in the framework of the project SA120004. We are grateful to Center of Scientific Computing, Espoo, for its computational resources.

*vehvilainen@iki.fi

[1] H. Kroto, J. Heath, S. O'Brien, and R. Smalley, Nature (London) **318**, 162 (1985).
[2] R. A. Freitas Jr., Biology and Medicine **1**, 2 (2005).
[3] A. Dillon and M. Heben, Appl. Phys. A **72**, 133 (2001).
[4] A. Züttel, Naturwissenschaften **91**, 157 (2004).
[5] Y. Kawazoe *et al.*, J. Mol. Graphics Modell. **19**, 270 (2001).
[6] H. Terrones and M. Terrones, New J. Phys. **5**, 126 (2003).
[7] S. Lee, L. An, Y. Lee, G. Seifert, and T. Frauenheim, J. Am. Chem. Soc. **123**, 5059 (2001).
[8] C. Liu *et al.*, Science **286**, 1127 (1999).
[9] Y. Ma, Y. Xia, M. Zhao, R. Wang, and L. Mei, Phys. Rev. B **63**, 115422 (2001).
[10] A. Dillon *et al.*, Nature (London) **386**, 337 (1997).
[11] Y. Okamoto, J. Phys. Chem. A **105**, 7634 (2001).
[12] H. Prinzbach *et al.*, Nature (London) **407**, 60 (2000).
[13] K. Whitener *et al.*, J. Am. Chem. Soc. **130**, 13996 (2008).
[14] O. Pupysheva, A. Farajian, and B. Yakobson, Nano Lett. **8**, 767 (2008).
[15] K. Komatsu, M. Murata, and Y. Murata, Science **307**, 238 (2005).
[16] G. Kresse and J. Furthmüller, Phys. Rev. B **54**, 11169 (1996).
[17] G. Kresse and J. Furthmüller, Comput. Mater. Sci. **6**, 15 (1996).
[18] J. P. Perdew, K. Burke, and M. Ernzerhof, Phys. Rev. Lett. **77**, 3865 (1996).
[19] P. Blochl, C. Forst, and J. Schimpl, Bulletin of Materials Science **26**, 33 (2003).
[20] H. Monkhorst and J. Pack, Phys. Rev. B **13**, 5188 (1976).
[21] G. Seifert, Solid State Ionics **168**, 265 (2004).
[22] K. Beardmore, R. Smith, A. Richter, and B. Mertesacker, J. Phys. Condens. Matter **6**, 7351 (1994).
[23] Y. Ferro, F. Marrinelli, and A. Allouche, Chem. Phys. Lett. **368**, 609 (2003).
[24] S. Casolo, O. M. Løvvik, R. Martinazzo, and G. F. Tandardini, J. Chem. Phys. **130**, 054704 (2009).
[25] F. Lin, E. S. Sørensen, C. Kallin, and A. J. Berlinsky, Phys. Rev. B **76**, 033414 (2007).
[26] F. Lin, J. Smakov, E. S. Sørensen, C. Kallin, and A. J. Berlinsky, Phys. Rev. B **71**, 165436 (2005).
[27] F. Lin and E. S. Sørensen, Phys. Rev. B **78**, 085435 (2008).
[28] E. Sanville and J. Bruno, J. Phys. Chem. B **107**, 8884 (2003).
[29] C. Lee, W. Yang, and R. G. Parr, Phys. Rev. B **37**, 785 (1988).
[30] P. O. Lehtinen, A. S. Foster, Y. Ma, A. V. Krasheninnikov, and R. M. Nieminen, Phys. Rev. Lett. **93**, 187202 (2004).
[31] P. O. Lehtinen, A. S. Foster, A. Ayuela, A. Krasheninnikov, K. Nordlund, and R. M. Nieminen, Phys. Rev. Lett. **91**, 017202 (2003).
[32] A. V. Krasheninnikov, P. O. Lehtinen, A. S. Foster, P. Pyykkö, and R. M. Nieminen, Phys. Rev. Lett. **102**, 126807 (2009).
[33] N. Park, M. Yoon, S. Berber, J. Ihm, E. Osawa, and D. Tománek, Phys. Rev. Lett. **91**, 237204 (2003).
[34] Y. Ma, P. O. Lehtinen, A. S. Foster, and R. M. Nieminen, Phys. Rev. B **72**, 085451 (2005).
[35] J. Zhou *et al.*, Nano Lett. **9**, 3867 (2009).
[36] W. Orellana, Phys. Rev. B **80**, 075421 (2009).
[37] G. Henkelman, B. P. Uberuaga, and H. Jonsson, J. Chem. Phys. **113**, 9901 (2000).
[38] D. Sheppard, R. Terrell, and G. Henkelman, J. Chem. Phys. **128**, 134106 (2008).
[39] J. O. Sofo, A. S. Chaudhari, and G. D. Barber, Phys. Rev. B **75**, 153401 (2007).
[40] D. C. Elias *et al.*, Science **323**, 610 (2009).